Physica B 406 (2011) 2453–2457

Contents lists available at ScienceDirect

Physica B

journal homepage: www.elsevier.com/locate/physb

A compact TOF-SANS using focusing lens and very cold neutrons

Masako Yamada [a,*], Yoshihisa Iwashita [a], Toshiji Kanaya [a], Norifumi L. Yamada [b], Hirohiko M. Shimizu [b], Kenji Mishima [b], Masahiro Hino [c], Masaaki Kitaguchi [c], Katsuya Hirota [d], Peter Geltenbort [e], Bruno Guerard [e], Giuliana Manzin [e], Ken Andersen [e], Jyotsana Lal [f], John M. Carpenter [g], Markus Bleuel [h], Shane J. Kennedy [i]

[a] ICR, Kyoto University, Gokasho, Uji, Kyoto 611-0011, Japan
[b] KEK, 1-1 Oho, Tsukuba, Ibaraki 305-0801, Japan
[c] KURRI, 2-1010 Kumatori, Osaka 590-0494 Japan
[d] RIKEN, 2-1 Hirosawa, Wako, Saitama 351-0198, Japan
[e] Institut Laue-Langevin, 6 Rue Jules Horowitz, B.P.156, F-38042 Grenoble Cedex 9, France
[f] Biosciences Division, ANL, IL 60439, USA
[g] APS Engineering Support Division, ANL, IL 60439, USA
[h] Reactor Institut Delft TU, Mekelweg 15, 2629 JB Delft, The Netherlands
[i] Bragg Institute, ANSTO, Lucas Heights, NSW 2234, Australia

ARTICLE INFO

Available online 8 December 2010

Keywords:
Focusing lens
Rot-PMSx
Pulsed neutron beams
TOF
High resolution
Compact instrument
VCN
Focusing-SANS

ABSTRACT

We are developing a high-resolution small angle neutron scattering instrument for very cold neutrons (VCN). Our concept includes a magnetic lens for focusing of the beam at the detector plane. The lens consists of one permanent-magnet sextupole array rotating outside another stationary sextupole array, to focus a pulsed white beam of neutrons. Thus the instrument operates in time of flight mode. The prototype magnetic lens has a bore of 15 mm diameter and length of 66 mm, producing a magnetic field gradient oscillating from 1.5×10^4 to 5.9×10^4 T/m^2, with frequency ≤ 25 Hz. A torque-canceling magnet around the lens suppresses the torque of rotation from the outer array to 1/3.

We have demonstrated the performance of the lens, over wavelength range from 30 to 48 Å, on the PF2-VCN beam line at the Institut Laue-Langevin, France. The focused beam image was the same size as the source, without chromatic aberration, with focal length of 1.14 m. We also studied the performance of this configuration for high-resolution SANS, in a compact geometry (just 5 m long). The measurable q range of this system was $0.009\ \text{Å}^{-1}\leq q\leq 0.3\ \text{Å}^{-1}$ or $0.004\ \text{Å}^{-1}\leq q\leq 0.08\ \text{Å}^{-1}$ for sample to detector distances of 100 and 465 mm, respectively. Here, we present the results of our lens characterization study along with the SANS results on a tri-block copolymer (F127 Pluronic) and on a stretched polymer blend (with the Shish-Kebab structure).

1. Introduction

We are developing a high resolution compact small angle neutron scattering instrument (SANS) utilizing a combination of pulsed white very cold neutron (VCN) beams and focusing magnetic lens [1–3]. We call this system VCN-f-SANS.

Small angle scattering (SAS) using neutrons or X-rays provide a powerful method for the elucidation of nano-scale structures. In recent decades this method has contributed greatly in the fields of polymer, biological and materials sciences, and continues to grow in popularity. Modern science presents many challenges for the extension of the method, in terms of larger scale correlations (greater than 1 μm), wider dynamic range (such as with hierarchical structures and complex chemical reactions) and higher resolution (in the case of nano-technology).

In SAS the scattering vector (q) is usually represented as

$$q = 2\pi \sin 2\theta/\lambda, \tag{1}$$

where 2θ and λ are the scattering angle and the de Broglie wavelength of radiation, respectively. By using longer wavelength radiation we can reach lower minimum scattering vector (q_{min}), and therefore larger size scales, and higher resolution (δq), due to increased scattering angle. We can further improve both q_{min} and δq by focusing the beam onto the plane of the detector, using a magnetic focusing lens, which produces no aberration due to scattering.

In order to widen the dynamic range we could extend the maximum scattering angle or we could use a wide range of wavelengths, using the time-of-flight (TOF) method, or we could do both.

* Corresponding author.
E-mail address: yamada@kyticr.kuicr.kyoto-u.ac.jp (M. Yamada).

0921-4526/$ - see front matter © 2010 Elsevier B.V. All rights reserved.
doi:10.1016/j.physb.2010.12.002

However, the TOF method is only compatible with beam focusing of the focusing power, which can be synchronized with the neutron wavelength to produce a constant focal length. In order to address emerging scientific demand all these enhancements must be arranged without seriously impacting on beam current (integrated flux at the sample position).

Our novel approach to address these challenges is to explore the VCN spectral range (20–80 Å). In doing so we recognize that 2θ is no longer small, and that the sample to detector distance must be substantially reduced, to a point quite close to the focus of the lens; so that the smaller size samples are measurable. The powerful permanent magnetic lens makes the total instrument very compact for the VCN spectrum. For example, the focal length of our prototype lens is just 0.5 m for a neutron wavelength of 40 Å.

2. Focusing pulsed white neutrons by rotating sextupole lens

When a neutron moves through a magnetic field gradient, its trajectory will be deflected due to interaction between its magnetic dipole moment and magnetic field B [4–6], which is described as

$$B = (1/2)g'(x^2+y^2), \quad (2)$$

where the beam axis is defined as z-axis, the perpendicular axes in the transverse plane are x- and y-axes and g' is the magnetic field gradient. For a polarized beam of neutrons in a sextupole magnetic field, neutrons which have spin parallel to the field are focused to a focal point and the others are defocused. A pulsed beam of white neutrons will be focused without significant chromatic aberration when the modulation of g' is synchronized with the beam pulse [1,2,6].

2.1. Configuration of sextupole magnet

The permanent-magnet sextupole magnet lens (rot-PMSx) is shown in Fig. 1. Essentially, it consists of one permanent-magnet sextupole array rotating outside another *stationary* sextupole array. The magnetic lens is composed of Nd–Fe–B sintered permanent magnet (NEOMAX [7]) in the extended-Halbach configuration [2,8]. There are six poles made of soft magnetic material, Permendur (Fe49–Co49–2V) was laminated with thickness 2.5 mm to suppress eddy currents and reduce the associated heating. Lamination reduced the temperature rise during operation from 29 to 18 °C [3].

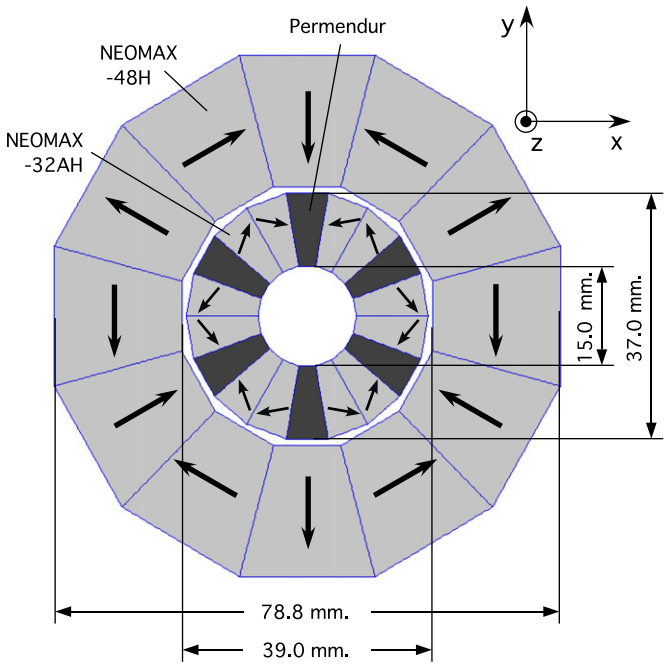

Fig. 1. Lens configuration at the maximum field gradient. Outer array is composed of 12 pieces of NEOMAX-48. Inner array is composed of 12 pieces of NEOMAX-32AH and 6 pieces of Permendur. Arrows show directions of magnetization.

The lens has a bore ($\varnothing$) of 15 mm, path length of 66 mm, variation of g' over range $1.5\times10^4\ \mathrm{T/m^2} \le g' \le 5.9\times10^4$, and operates at frequency up to 25 Hz. The strongest magnetic field at the inner surface of the bore almost saturates and is very strong (1.6 T) compared to electromagnets or superconducting-magnets. At this field strength, the focal length is just 0.5 m for 40 Å neutrons.

The outer array is driven by a 1.5 kW electric motor, through a belt drive. Volume of the entire system is quite compact, with a footprint of 370 × 300 mm, and total height of 435 mm (see Fig. 3 in following Section 2.3).

2.2. Torque canceller

The torque produced by rotation of the outer array of magnets is excessive, and makes high frequency rotation difficult [3]. So the lens incorporates a torque-canceling (TC) magnet array mounted co-axially around the focusing sextupole magnet and rotating with half period phase shift to suppress the torque experienced by the motor. As shown in Fig. 2, the measured torque is suppressed by 2/3 by the torque canceler.

2.3. Proof of principle of white beam focusing

The evaluation of the ability of the lens to focus a white polarized neutron beam was performed on the PF2-VCN beam line [1] at the Institut Laue-Langevin [9]. In this experiment, the phase of the magnetic field gradient modulation was synchronized with the wavelength spectrum of the neutron beam pulse, so that the focal length remains constant over the entire pulse. The picture of the magnetic lens in this experiment is shown in Fig. 3.

For a schematic of the configuration used here we can refer to Fig. 4, which differs only in the respect that a sample for a SANS experiment is placed between the lens and detector. For the focusing evaluation and SANS1 the detector was placed at focal point, while the focal point falls between the sample and the detector for SANS2 (see Table 1 in Section 3).

The continuous VCN beam from the reactor is pulsed by a single disk chopper with a 60 ms period and 1 ms opening time. The beam is then polarized by a polarizing supermirror (with m=2.3 and

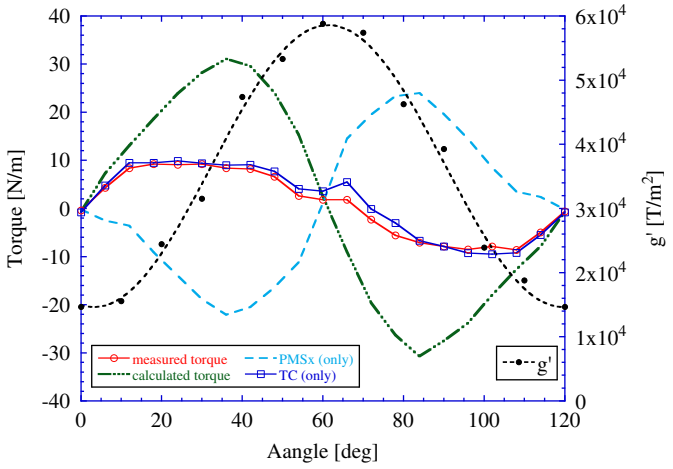

Fig. 2. Measured torques for rotation of outer array at magnet with TC, without TC and TC or rot-PMSx. The magnetic field gradient is shown as well.

incident angle of 6.8°). The supermirror also serves as a high energy neutron filter, cutting off neutrons of wavelength <30 Å. The polarized beam goes through a circular aperture ($\varnothing_1=3$ mm), which is the source aperture. The lens aperture ($\varnothing_2=14$ mm) is fixed on the entrance of the lens. Magnification of this optical arrangement is one. The distance (L_1) from source aperture to lens was equal to the distance (L_2) from lens to detector, and twice the focal lens of the lens, i.e. $L_1=L_2=2f=2275$ mm. Thus the magnification was one. The beam was observed at the image by a two-dimensional ^{3}He position sensitive detector, with area 80×80 and a 2 mm resolution [10].

The measured beam profiles at the image, with and without lens, for selected wavelengths, are shown in Fig. 5. Note that the beam shape is ellipsoidal with and without lens. This illustrates the difficulty of beam alignment at these wavelengths and over a broad wavelength range. This effect is entirely due to gravity. It is not possible to transmit such a broad wavelength range through the pair of apertures ($\varnothing_1$ and $\varnothing_2$) without spectral losses, so the lens has no effect on the eccentricity of the beam shape. Here we reached a compromise favouring the longer wavelengths.

The observed beam profile was fitted with a two-dimensional Gaussian distribution function, and we equated the beam size (FWHM) to $2\times\sqrt{2\ln(2)\sigma^2}$, where σ^2 is the variance of the Gaussian. When the lens was in operation the measured image width at the detector matched the source width over a wavelength range from 30 Å $\le\lambda\le$ 48 Å. As discussed above, the image height was reduced from the source height due to gravitational losses. By comparing the beam area in the absence of the lens to beam area when the lens is in operation, we can obtain the flux gain of the focusing lens. Here we determine the flux gain to be about 30 over the entire wavelength range. This gain was achieved with imperfect beam polarization ($<70\%$) and limited detector resolution (3–4 mm). We expect that substantially higher gains could be achieved with a smaller source, higher polarization and higher detector resolution.

Thus we have demonstrated that the lens focuses over an exceptionally broad wavelength range ($\delta\lambda/\lambda\sim50\%$) without chromatic aberration. Nevertheless, we observed that the pulsed, polarized VCN beam suffers from very low intensity (see Fig. 6), particularly at longer wavelengths. We expect that losses due to gravity and air scattering are partly responsible for the low intensity.

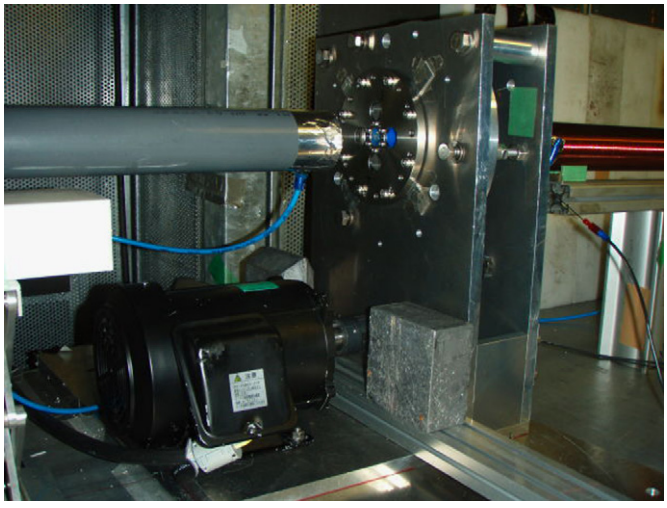

Fig. 3. Rotating sextupole lens in operation at (PF-2) VCN beam line.

3. Demonstration of VCN-f-SANS

After confirming that the VCN beam was focused as desired by the rotating lens, we demonstrated the performance of the system for high resolution SANS (VCN-f-SANS). The setup for SANS, which is almost the same as that discussed earlier, is shown in Fig. 4. The distances between each device are listed in Table 1.

Referring to Table 1, the essential difference between SANS1 and SANS2 configurations is in q-range and q-resolution, i.e. SANS1 has larger q range and SANS2 has higher resolution.

To increase flux on sample in the SANS measurements, the first aperture ($\varnothing_1$) was increased from 3 to 5 mm and the chopper disk opening time was increased from 1 to 3 ms. Also for the SANS measurements, a detector of area 260×260 mm^2 was used [10] to cover a wider angular range.

3.1. Results for Pluronic F127

The first sample discussed is a well characterized tri-block copolymer Pluronic F127, $((PEO)_{100}(PPO)_{65}(PEO)_{100})$. This is a non-ionic macromolecular surfactant that is used commercially as an anti-foaming agent. It has been the subject of intense research because of its series of temperature and concentration dependent phase transitions [11–13].

At temperatures close to ambient, each unimer self-aggregates into spherical micelles of Pluronic F127 with the core dominated by PPO and a corona dominated by the hydrated PEO blocks. Above a critical concentration and within a temperature range ($\sim$13–56 °C),

Table 1
Distances of VCN-f-SANS demonstration experiment.

	SANS1	SANS2
$a+b$ (mm)	260	260
L_1 (mm)	2265	2265
L_2 (mm)	2265	2565
L_3 (mm)	100	465
total length (mm)	4790	5090

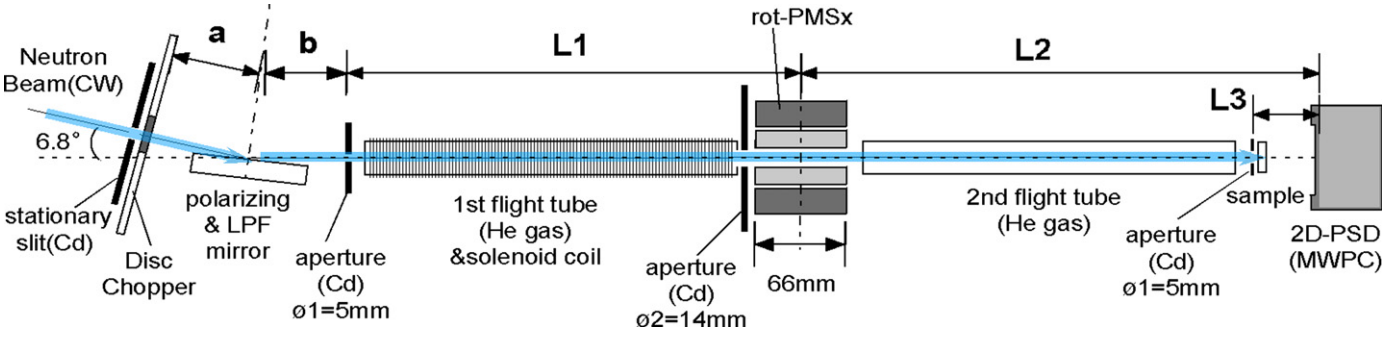

Fig. 4. Experimental set up for VCN-f-SANS.

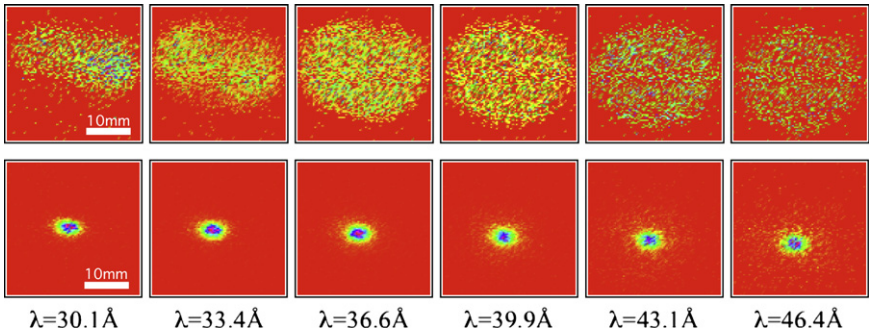

Fig. 5. Beam images at focus point depending on wavelength (down) compared with ones without lens (up). Beam flux gain is about 30 at all wavelengths.

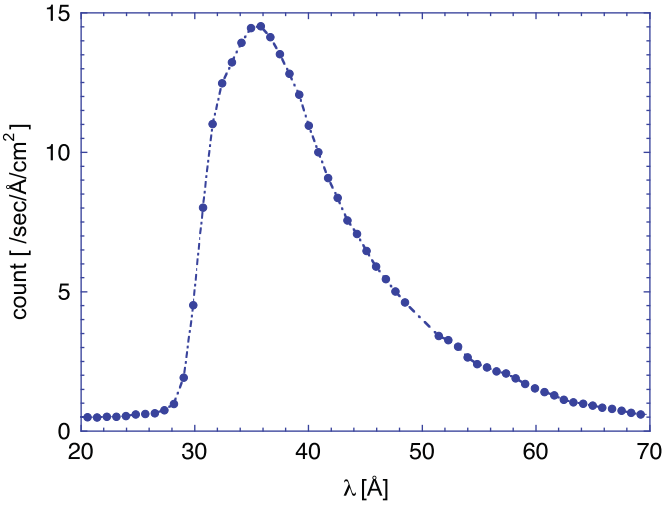

Fig. 6. Beam profile at focus point.

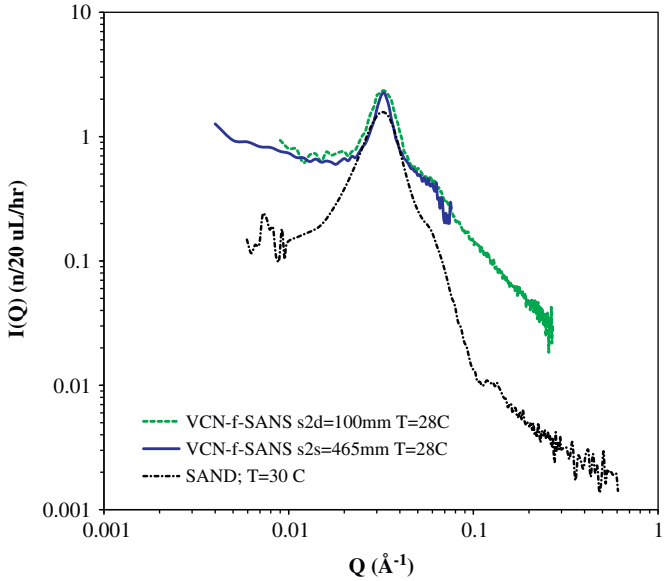

Fig. 7. VCN-f-SANS for 15 wt% Pluronic in D_2O (28 °C), compared with SAND at IPNS (30 °C).

the tri-block copolymer's spherical micelles are close packed into a cubic phase.

The sample was a 1 mm thick solution of 15 wt% Pluronic F127 in D_2O. Our measurements at 4, 28, 51 and 70 °C spanned the unimer, close packed micelle and liquid micelle phases.

As an example of the results obtained, the measured scattering function $I(q)$ versus scattering vector (q) at 28 °C in both SANS1 and SANS2 configurations are plotted in Fig. 7, along with measurements taken on an identical sample at 30 °C by the *SAND* instrument at IPNS (Argonne National Laboratory). Each measurement at VCN-f-SANS were performed for 5 h, while for 8 h in the measurement at SAND. In order to correct for the different sample thickness, beam size and measurement time of the *SAND* measurement $I(q)$ has been corrected to neutrons per 20 μl of sample per hour measurement time. The minima and maxima of scattering vectors for each measurement are compared in Table 2.

Several features of the VCN-f-SANS method are immediately apparent. The q range in SANS1 is narrower but approaches that of the *SAND* measurement, whereas SANS2 reaches much lower q at the expense of a great reduction in high q. The peak in both of the VCN-f-SANS patterns is sharper than in the *SAND* pattern, with SANS2 providing the highest resolution (δq).

VCN-f-SANS also produced more intense scattering, albeit with much higher background. These features are most likely explained by the fact that the VCN-f-SANS sample is effectively a much stronger scatterer, due to the strong dependence of scattering power on neutron wavelength. In this case the degradation (high background) due to multiple scattering outweighs the advantage of stronger scattering. We estimate the optimum sample thickness for Pluronic to be between 0.1 and 0.2 mm.

Table 2
Measured configurations of VCN-f-SANS and SAND.

SANS system	q_{min} (Å^{-1})	q_{max} (Å^{-1})
VCN-SANS 1	0.009	0.3
VCN-SANS 2	0.004	0.08
SAND (IPNS)	0.007	0.5

Although the experimental arrangement was far from ideal, these results are very encouraging for pushing further with this technique in the future.

3.2. Results for Shish-Kebab

We also performed a SANS measurement on an elongated blend of low molecular weight (LWM) deuterated (dPE) and high molecular weight (HMW) hydrogenated polyethylene (hPE; 99/1 wt%). When this polymer blend is elongated it forms the so called *Shish Kebab* structure [14]. This structure consists of a long central cores (*shish*) aligned along the elongation direction surrounded by lamellar crystals (*kebabs*), which are composed of HMW-hPE or LMW-dPE, respectively. It has been shown that these polymer blends can be elongated to many times their initial length.

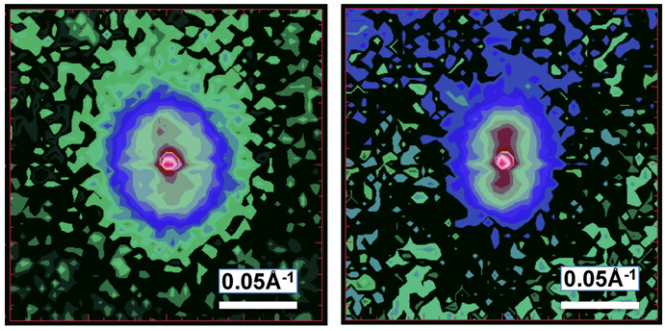

Fig. 8. Two-dimensional SANS pattern in q-space for non-elongated (left) and elongated (right) samples.

Fig. 8 shows the measured scattering function $I(q)$ versus scattering vector q of elongated (elongated by a factor of 2) and non-elongated polymer blends. These measurements were performed in the SANS1 configuration.

The sample aperture diameters, sample thicknesses and measurement times were 4 and 2 mm, 0.8 and 0.6 mm and 140 and 390 min for non-elongated and elongated samples, respectively. The anisotropy shown by the non-elongated sample is due to some level of non-uniformity inherent in the process of producing the sample in sheet form. This could be suppressed by annealing after production. As expected, the elongated sample shows enhanced anisotropy. The length of the central cores extends into the micron range, which is clearly beyond the range of the current measurements. Nonetheless, these results are consistent with the preceding experiments and show the potential of VCN-f-SANS to measure two-dimensional scattering patterns on small samples of anisotropic materials.

4. Discussion

Our results clearly demonstrate the potential of the VCN-f-SANS method as depicted in Fig. 4. Several improvements are envisaged that could improve performance by orders of magnitude. Amongst these is reduction in multiple scattering, which was relatively high in these samples, i.e. transmission of the Pluronic, non-elongated Shish-Kebab and elongated Shish-Kebab were 26%, 46% and 73%, respectively. We could estimate and suppress this problem by choosing optimum path lengths for the samples in the future. This will allow us to work with small sample volumes with VCN and to our great advantage, use relatively small samples similar to the ones used with X-ray beams.

In the demonstration of beam focussing the flux losses caused by gravity were substantial. To eliminate this beam loss, the beam could be reflected upwards to the vertical direction at the polarizing supermirror (see Fig. 4) so that the beam current over the whole wavelength band at the lens and sample would become maximum. Details are discussed in Ref. [1]. Vertical configuration would suppress aberration caused by gravity when longer and wider wavelength range neutron beams are utilized.

Finally the limited q range is largely a result of the limited detector size. A detector that subtends a much higher angular range could allow maximum $q_{max} \sim 0.5$ Å^{-1}, which would then be comparable to many existing SANS.

References

[1] M. Yamada, et al., Nucl. Instr. and Meth. A (2010). doi:10.1016/j.nima.2010.06.259.
[2] Y. Iwashita, et al., Nucl. Instr. and Meth. 73 (2008) 586.
[3] M. Yamada, et al., Physica B 404 (2009) 2646.
[4] H.M. Shimizu, et al., Physica B 241–243 (1998) 172.
[5] H.M. Shimizu, et al., Nucl. Instr. and Meth. A 430 (1999) 423.
[6] J. Suzuki, et al., Nucl. Instr. and Meth. A 529 (2004) 120.
[7] NEOMAX. 〈http://www.neomax-materials.co.jp/〉.
[8] M. Kumada, et al., IEEE Trans. Appl. Supercond. AS-14 (2) (2004) 1287.
[9] PF2 Beam Line at ILL. 〈http://www.ill.eu/instruments-support/instruments-groups/instruments/pf2/〉.
[10] The 80 × 80 mm detector is known as *bidim*-80 and the 260 × 260 mm detector is known as *bidim*-26. B. Guerard, G. Manzin, Institute Laue-Langevin, Private Communication.
[11] R.K. Prudfhomme, et al., Langmuir 12 (1996) 4651.
[12] J.S. Pedersen, M.C. Gerstenberg, Macromolecules 29 (1996) 1363.
[13] J.S. Pedersen, Adv. Colloid Interface Sci. 70 (1997) 171.
[14] T. Kanaya, et al., Macromolecules 40 (2007) 3650.